

Cluster Monte Carlo: Scaling of Systematic Errors in the 2D Ising Model

Lev N. Shchur † and Henk W.J. Blöte ‡

†Landau Institute for Theoretical Physics, 117940 GSP-1 Moscow V-334, Russia

‡Laboratory of Applied Physics, Delft University of Technology, P.O. Box 5046, 2600 GA Delft, The Netherlands

We present an extensive analysis of systematic deviations in Wolff cluster simulations of the critical Ising model, using random numbers generated by binary shift registers. We investigate how these deviations depend on the lattice size, the shift-register length, and the number of bits correlated by the production rule. They appear to satisfy scaling relations.

The main advantage of cluster Monte Carlo algorithms is that they suppress critical slowing down [1,2]. For this reason, cluster algorithms are being explored extensively [3]. This has even led to the construction of special-purpose processors using the Wolff cluster algorithm [4,5].

The problem of generating random numbers of sufficient quality is known to be complicated since the first computer experiments [6]. Many of the widely used algorithms are of the shift-register (SR) type [7]. These are extremely fast [8], can be implemented simply in hardware [9,10] and produce 'good random numbers' with an extremely long period [7].

Ferrenberg et al. [11] found that the combination of the two most efficient algorithms (the Wolff cluster algorithm and the shift-register random-number generator) produced large systematic deviations for the 2D Ising model on a 16×16 lattice (see also [12]). Also random-walk algorithms appeared to be sensitive to effects due to the random-number generator [13].

Remarkably, we did not find visible deviations in simulations [4,14] performed on the special-purpose processor with the Wolff algorithm and a Kirkpatrick-Stoll random-number generator for lattices larger than 256×256 .

Motivated by this paradoxical situation, we made an extensive analysis of this problem using SGI workstations at the Delft University and a DEC AXP 4000/620 server at the Landau Institute. A total of about two thousands hours of CPU time was spent.

We find several interesting facts. First, the maximum deviations occur at lattice sizes for which average Wolff cluster size coincides with the length p of the SR.

Second, the deviations obey scaling laws with respect to p : they can be collapsed on a single curve. This opens the possibility to predict the magnitude of the systematic errors in a given quantity, depending on the lattice size, the shift-register length and, to some extent, also on the number of terms in production rule.

Third, the deviations change sign when we invert the

range of the random number: $x \rightarrow 1 - x$. This provides a simple test, in two runs only, for the presence of systematic errors.

Finally, we introduce a simple 1D random-walker model explaining how the correlations in the SR lead to a bias in Monte Carlo results.

As a first step in understanding the results, it is natural to compare the length scales associated with the Monte Carlo process and the random generator. The first characteristic length is the mean Wolff cluster size $\langle c \rangle$. The second characteristic length is the size p of the shift register. The production rule

$$x_n = x_{n-p} \oplus x_{n-q}, \quad (1)$$

where \oplus is the 'eXclusive OR' operation, leads to three-bit correlations over a length p . So, it not surprising that the largest deviations occur at the lattice size L_{\max} for which these two lengths coincide. Since the mean Wolff cluster size behaves [2] as the magnetic susceptibility χ , we expect at criticality that

$$p \propto \chi \propto L_{\max}^{\gamma/\nu}, \quad (2)$$

where γ and ν are the susceptibility and correlation length exponents respectively.

We performed Wolff simulations of the 2D Ising model at criticality, using SR with feed-back positions $(p, q) = (36, 11), (89, 38), (127, 64)$ and $(250, 103)$ as listed in Ref. [15] and references therein. For each pair (p, L) we took 100 samples of 10^6 Wolff clusters. Thus we determined the coefficient in Eq. (2): $p = 1.09(1) L_{\max}^{7/4}$. Here, and below, the numbers in parentheses indicate the statistical errors.

The results for the energy deviations $\delta E \equiv \langle E/E_{\text{ex}} - 1 \rangle$ are plotted in Fig. 1. The exact results are taken from Ref. [16]. The maximum deviations occur at $L = 7, 12, 15$ and 22 respectively, in agreement with Eq. (2). The inset in Fig. 1 displays the maximum deviations of the energy δE_{\max} as a function of the shift-register length. A fit yields $\delta E_{\max} \propto p^{-0.88(2)}$.

The resulting data collapse for the scaled deviations $\delta \tilde{E} \equiv p^{0.88} \delta E$ is shown in Fig. 2 versus the scaled system size $\tilde{L} \equiv p^{-0.43(5)} L$. The linear decay on the right obeys $\delta \tilde{E} \propto \tilde{L}^{-0.84(4)}$.

If the data for $L > p^{4/7}$ keep following the linear trend in Fig. 2, the maximum possible deviations can be described by relation

$$\delta E \lesssim 0.3 L^{-0.84} p^{-0.52}. \quad (3)$$

The results for (127,64) do not fit the curve well. This is no surprise because shift registers with (p,q) close to powers of 2 are known [17] to produce relatively poor random numbers.

Similarly, we sampled the deviation of the specific heat C . Fig. 3 shows scaled deviations $\delta\tilde{C} \equiv p^{0.51(2)}\delta C$ versus the scaled system size which is the same as for δE . For large \tilde{L} this curve behaves as $\delta\tilde{C} \propto \tilde{L}^{-0.21(2)}$. The deviations satisfy

$$-\delta C \lesssim 0.85 L^{-0.21} p^{-0.42} \quad (4)$$

but they can also be described in terms of a logarithm of L plus a constant.

Fig. 4 shows analogous results for the dimensionless ratio $Q = \langle m^2 \rangle^2 / \langle m^4 \rangle$, which is related to the Binder cumulant [18], using $\delta\tilde{Q} = \delta Q p^{0.60(1)}$ along the vertical scale. On the right hand side the data behave as $\delta\tilde{Q} \propto \tilde{L}^{-0.45(5)}$. Extrapolation leads to

$$\delta\tilde{Q} \lesssim 0.244 L^{-0.45} p^{-0.41}. \quad (5)$$

In order to explain the origin of the observed deviations, we present a simple model that captures the essentials of the Wolff cluster formation process. This model simulates a directed random walk in one dimension [19]. At discrete times, the walker makes a step to the right with probability μ ; otherwise the walk ends. The probability to visit precisely n consecutive nodes is

$$P_{\text{ex}}(n) = \mu^{n-1} (1 - \mu). \quad (6)$$

Now, we simulate this model using a SR random-number generator. Each walk starts directly after completion of the preceding one, without skipping any random numbers. First, we use the 'positive' condition $x_n \geq \mu$ for stopping. Thus, the random number at start always fulfills the condition $x_0 \geq \mu$, which ended the preceding walk.

In the simplest case $\mu = 1/2$, only the leading bit affects this condition. As long as the walk proceeds, the leading bits of the random numbers x_n are zero. After $p - 1$ successful moves, the SR algorithm will produce a number x_p with the leading bit equal to 1. Thus the walker cannot visit more than p nodes.

A probabilistically equivalent condition for stopping is the 'negative' condition $x_n < 1 - \mu$. Then, the leading bit of x_0 must be 0, and for x_n ($n \geq 1$) it is 1 until the walk ends. The walk cannot stop at the $n = p$, since $x_p \oplus x_{p-q} = 0 \oplus 1 = 1$.

One can calculate the deviation from the exact value of $P(n)$ at $n = p$, $n = p + q$ and at all linear combinations of numbers p and q . The detailed analysis will appear elsewhere [19] and here we only mention that the probability deviation $\delta P(n) = (P_{\text{comp}}(n) - P_{\text{ex}}(n)) / P_{\text{ex}}(n)$ at $n = p$ for the positive condition is equal to $(1 - \mu) / \mu$. It is important that a deviation, even at only one point $n = p$,

results in a deviation of the probability function for the points $n > p$ by $\delta P(n) = (2\mu - 1)^2 / \mu^4 - 1 < 0$. The deviations at the 'resonances' $n = ip + jq$ ($i = 1, 2, \dots$ and $-i < j < i$) are positive and lead to negative deviations of the next points.

Thus, in the case of the positive condition, most of the $\delta P(n)$ are negative. In the case of the negative condition, $\delta P(n)$ is negative for $n = p 2^k$ ($k = 0, 1, 2, \dots$); this results in positive deviations for the following points.

In effect, this replaces the probability μ by a new 'effective' probability μ^* , with $\mu^* > \mu$ for the positive condition and $\mu^* < \mu$ for the negative condition for most $n > p$. This provides a qualitative explanation of the deviations in Wolff simulations. The completion of a Wolff cluster is strongly correlated with the value of the random numbers used at that time. Thus, the three-bit correlations generated by the production rule lead to two-bit correlations in the following p random numbers. In particular when the mean Wolff cluster size is about p , one may expect serious deviations in the calculated quantities.

When one replaces the positive by the negative condition, in effect the three-bit correlation is inverted. Thus, one expects a change of sign of the systematic errors. We confirmed this for the 2D Ising model.

A simple modification of the SR (1) is to use only one out of every m random numbers generated by the production rule [11,12]. If $m = 2^k$, $k = (1, 2, \dots)$ this will lead to the same production rule (1). For $m = 3$ and, as an example, for SR (36,11) the resulting production rule is (36,24,12,11): a 5-point production rule, i.e. $x_n = x_{n-36} \oplus x_{n-24} \oplus x_{n-12} \oplus x_{n-11}$. However, the lowest-order correlations of the resulting random numbers do not occur at $n = p = 36$, but at $n = 48$ because the production rule is equivalent with a 4-point one, namely (48,23,11) [20]. The effect due to 4-point correlations appears to dominate over the 5-bit effects for $\mu > 1/2$. The deviations $\delta P(n)$ of Eq. (6) resemble those for a 3-point production rule. But for μ close to 1 they stand out only at $n = 48 k$, $k = 1, 2, \dots$, and not at linear combinations of other magic numbers. Their sign is the same for the positive and negative conditions because the 4-point rule correlates an even number of bits).

Next, we investigated these 4-bit effects in the case of Wolff simulations, using every third number produced by the rules (36,11) and (89,38), and runs of 10^9 clusters. The deviations obey the same scaling laws, but the amplitudes are about 20 times smaller for each of the quantities E , C and Q , in accordance with the behavior of the 1D model (see the asterisks in Fig. 2).

For $m = 5$ - using only every 5-th number [11] - the effective production rule correlates 5 bits [20]. It leads to deviations in 1D model, in particular at $n = pk$, $k = 2^i$. They are less than for the SR of Eq. (1) [19].

Very long simulations, using 100 samples $\times 10^7$ Wolff steps for $m = 5$, show that the deviations are even smaller

than for $m = 3$. Table I displays data for SR (36,11) and (89,38) at lattice sizes $L = 7$ and $L = 12$, respectively. Similar data are included for $m = 3$ and for $m = 1$.

So, we propose, in addition, that the systematic deviations of 2D Ising Wolff simulations are described by Eqs. (3-5) for all SR-type algorithms, but the coefficients should be corrected with a factor of roughly $10^{-(m_c-3)}$, where m_c is the number of bits correlated by the production rule.

A preliminary analysis [21] confirms relation (2) also for the 3D Ising model. The deviations can also be collapsed on universal curves, but the exponents and amplitudes differ from the 2D case.

We conclude that the 1D model provides a useful way for the analysis of random numbers, in particular for the detection of harmful correlations in SR sequences. The errors in Wolff simulations induced by these correlations satisfy scaling relations which have a considerable significance for large-scale Wolff simulations. For instance, they confirm that in recent simulations [14] of the random bond Ising model with lattice sizes L greater than 128, the bias due to the (250,103) Kirkpatrick-Stoll rule was less than the statistical errors.

As explained above, 3-bit correlations in a SR production rule lead to 2-bit correlations in the first p random numbers used for the construction of a new Wolff cluster. If the size of the latter grows large in comparison with p , the 2-bit effect will decrease because the amount of correlation contained in the first p numbers remains finite. Indeed, this is in agreement with the power-law decay on the right-hand sides of Figs. 2-4. Although 3-bit effects seem to be much smaller in the cases (L, p) investigated by us, there is no reason to believe that they are absent. Thus, eventually they are expected to end the aforementioned power-law decay.

ACKNOWLEDGMENTS

We are much indebted to J.R. Heringa for contributing his valuable insight in the mathematics of shift-register sequences. We acknowledge productive discussions with A. Compagner, S. Nechaev, V.L. Pokrovsky, W. Selke, Ya.G. Sinai, D. Stauffer and A.L. Talapov. L.N.S. thanks the Delft Computational Physics Group, where the most of the work has been done, for their kind hospitality. This work is partially supported by grants RFBR 93-02-2018, NWO 07-13-210, INTAS-93-211 and ISF MOQ000.

- [2] U. Wolff, Phys. Rev. Lett. **62**, 361 (1989).
- [3] D. Stauffer, ed., *Annual Reviews of Comp. Physics I* (World Scientific, 1994).
- [4] A.L. Talapov, L.N. Shchur, V.B. Andreichenko, and V.I. Dotsenko, Mod. Phys. Lett. B, **6**, 1111 (1992).
- [5] A.L. Talapov, H.W.J. Blöte and L.N. Shchur, Pis'ma v ZhETF **62**, 157 (1995); JETP Lett. **62**, 174 (1995).
- [6] D.E. Knuth, *The Art of Computer Programming* (Addison-Wesley, 1981), Vol. 2.
- [7] S.W. Golomb, *Shift Register Sequences* (Holden-Day, San-Francisco, 1967).
- [8] S. Kirkpatrick and E. Stoll, J. Comp. Phys. **40**, 517 (1981).
- [9] A. Hoogland, J. Spaa, B. Selman, and A. Compagner, J. Comp. Phys. **51**, 250 (1983).
- [10] A.L. Talapov, V.B. Andreichenko, V.I. S. Dotsenko, and L.N. Shchur, JETP Lett. **51**, 182 (1990).
- [11] A.M. Ferrenberg, D.P. Landau, and Y.J. Wong, Phys. Rev. Lett. **69**, 3382 (1992).
- [12] W. Selke, A.L. Talapov and L.N. Shchur, JETP Lett. **58**, 665 (1993); K. Kankaala, T. Ala-Nissilä and I. Vattulainen, Phys. Rev. E **48**, R4211 (1993); P.D. Coddington, Int. J. Mod. Phys. **C 5**, 547 (1994).
- [13] P. Grassberger, Phys. Lett. A **181**, 43 (1993).
- [14] A.L. Talapov and L.N. Shchur, Europhys. Lett. **27**, 193 (1994); A.L. Talapov and L.N. Shchur, J. Phys. C: Condens. Matter **6**, 8295 (1994).
- [15] J.R. Heringa, H.W.J. Blöte and A. Compagner, Int. J. Mod. Phys. C **3**, 561 (1992).
- [16] A.E. Ferdinand and M.E. Fisher, Phys. Rev. **185**, 832 (1969).
- [17] A. Compagner and A. Hoogland, J. Comp. Phys. **71**, 391 (1987).
- [18] K. Binder, Z. Phys. B **43**, 119 (1981).
- [19] L.N. Shchur, H.W.J. Blöte and J.R. Heringa (unpublished).
- [20] J. Heringa and A. Compagner, private communication (1996).
- [21] L.N. Shchur and H.W.J. Blöte, unpublished (1996).

TABLE I. Deviations of energy δE , specific heat δC and ratio δQ . The statistical error in the last decimal place is shown between parentheses. We used a shift-register length $p = 36$ for $L = 7$ and $p = 89$ for $L = 12$. The bias appears to depend strongly on the number m_c of bits correlated by the production rule.

L	m_c	δE	δC	δQ
7	3	0.007797 (10)	-0.094307 (52)	0.014442 (10)
7	4	-0.000356 (13)	0.005894 (69)	-0.000720 (14)
7	5	-0.000060 (11)	0.001122 (60)	-0.000133 (15)
12	3	0.003345 (9)	-0.066797 (65)	0.009577 (13)
12	4	-0.000149 (15)	0.003296 (79)	-0.000274 (18)
12	5	-0.000003 (11)	0.000136 (89)	-0.000009 (15)

[1] R.H. Swendsen and J.-S. Wang, Phys. Rev. Lett. **58**, 86 (1987).

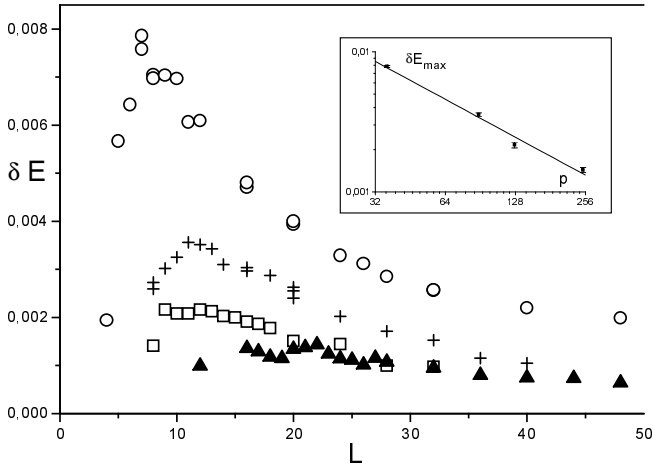


FIG. 1. Energy deviations δE for several SR, namely (36,11): \circ ; (89,38): $+$; (127,64): \square ; and (250,103): \blacktriangle . The inset shows the maximum value of δE as a function of p .

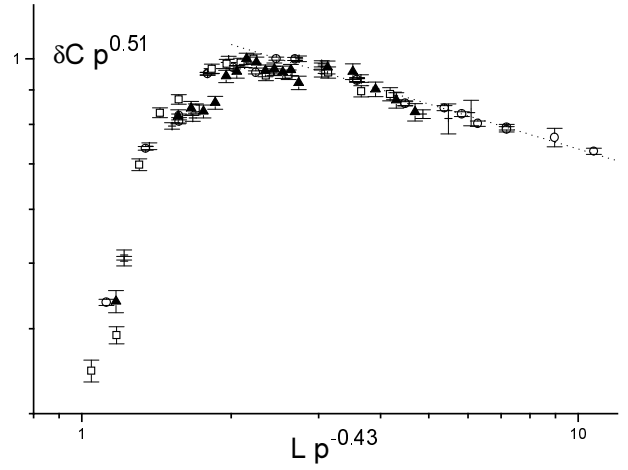


FIG. 3. Scaled deviation of specific heat δC versus the scaled system size, for several SR. The symbols are defined in the caption to Fig. 1.

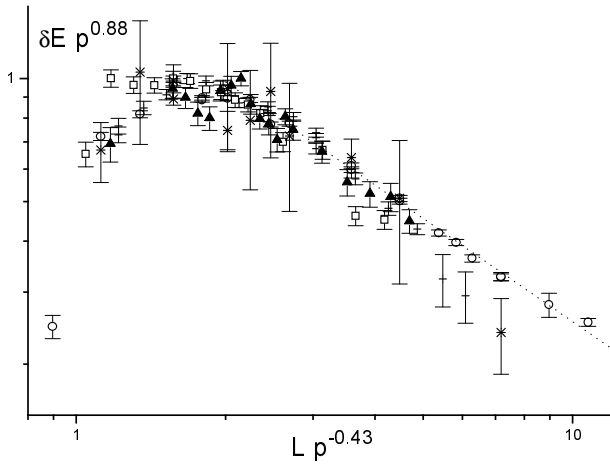


FIG. 2. Scaled deviation of the energy δE versus the scaled system size, for several SR. The symbols are defined in the caption to Fig. 1.

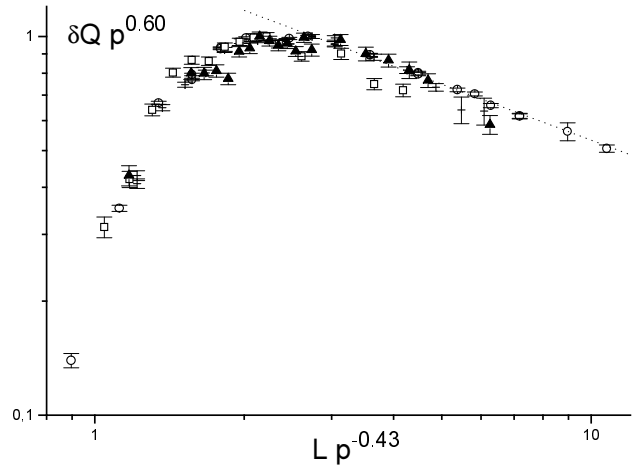


FIG. 4. Scaled deviation of dimensionless ratio δQ versus the scaled system size, for several SR. The symbols are defined in the caption to Fig. 1.

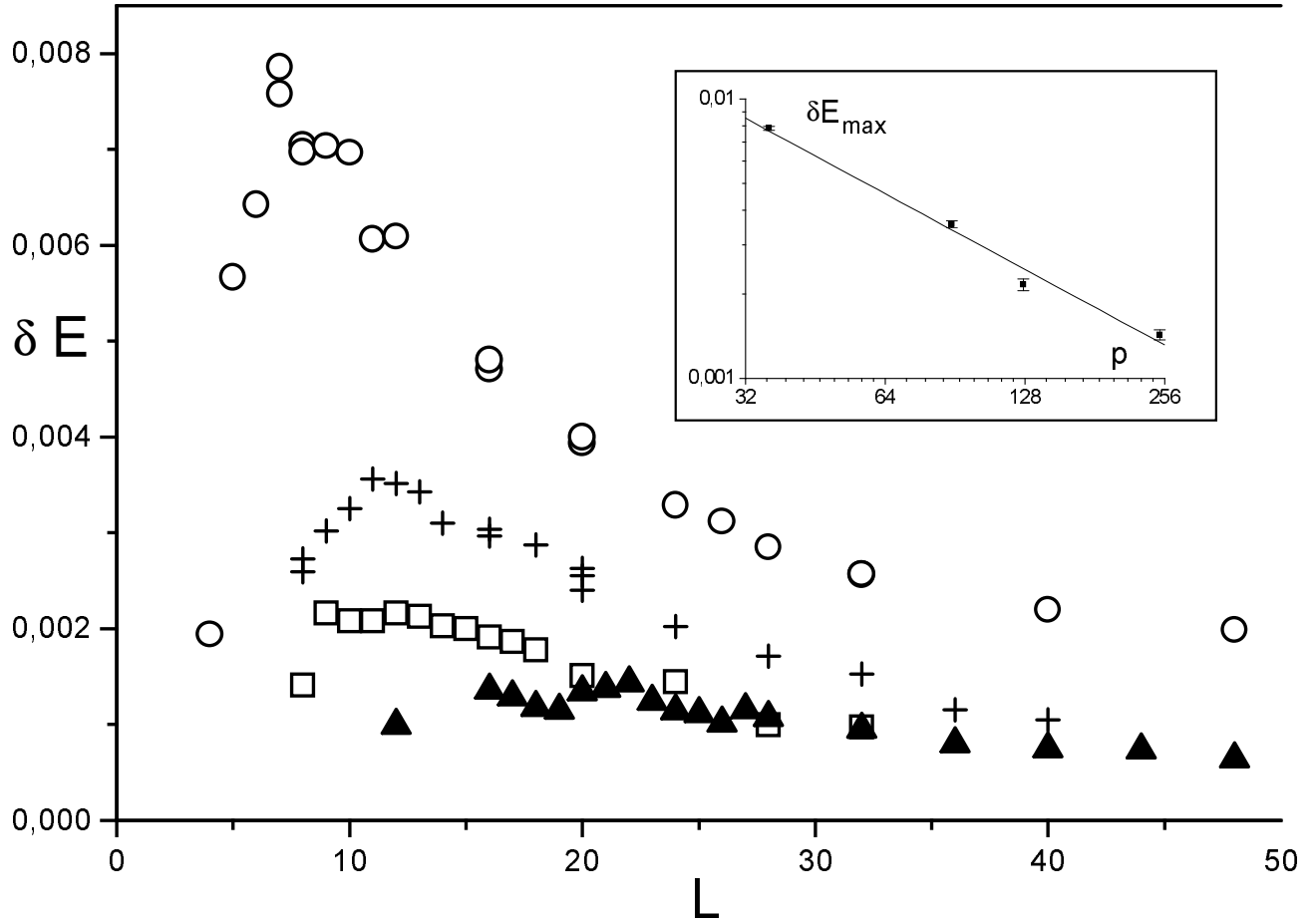


FIG. 1. Energy deviations δE for several SR, namely (36,11): \circ ; (89,38): $+$; (127,64): \square ; and (250,103): \blacktriangle . The inset shows the maximum value of δE as a function of p .

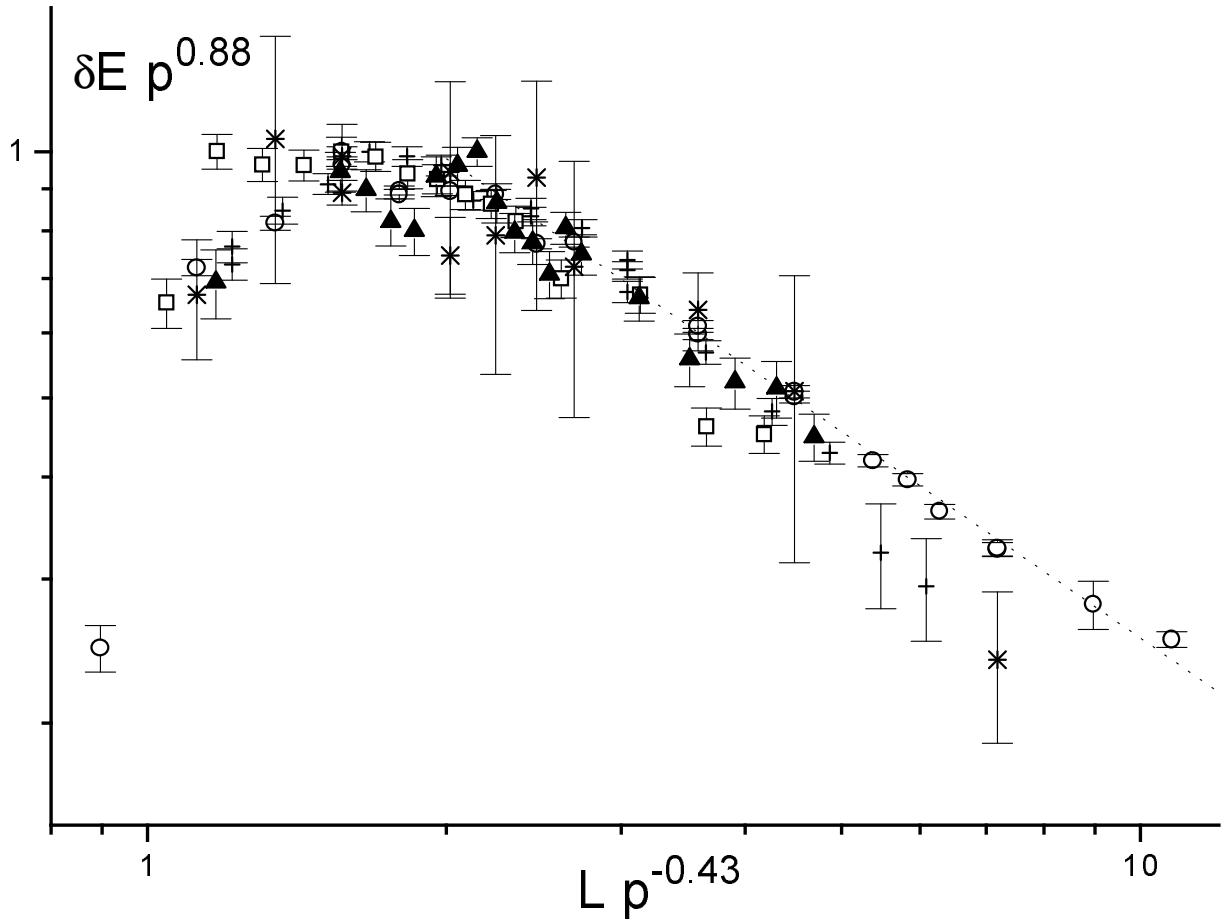


FIG. 2. Scaled deviation of the energy δE versus the scaled system size, for several SR. The symbols are defined in the caption to Fig. 1.

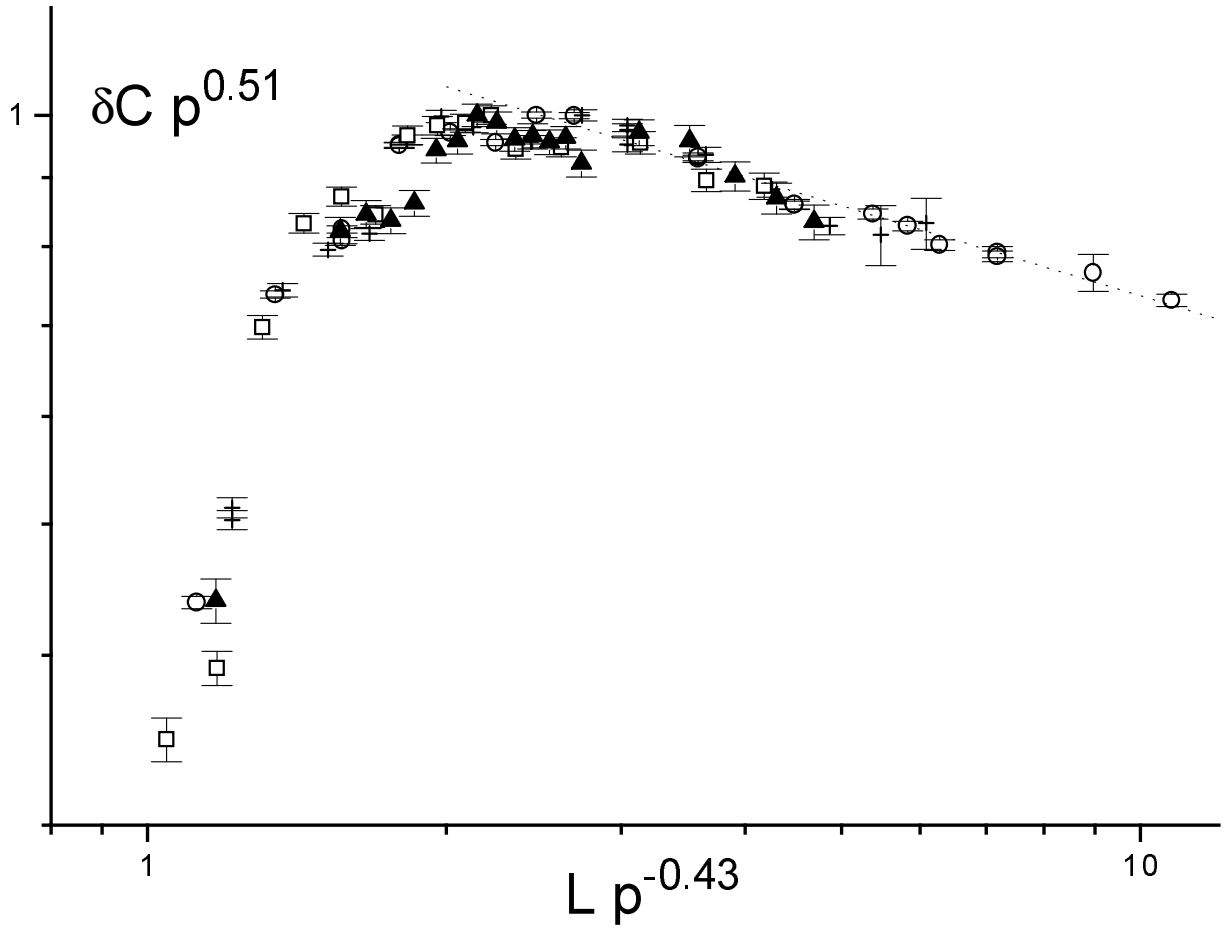


FIG. 3. Scaled deviation of specific heat δC versus the scaled system size, for several SR. The symbols are defined in the caption to Fig. 1.

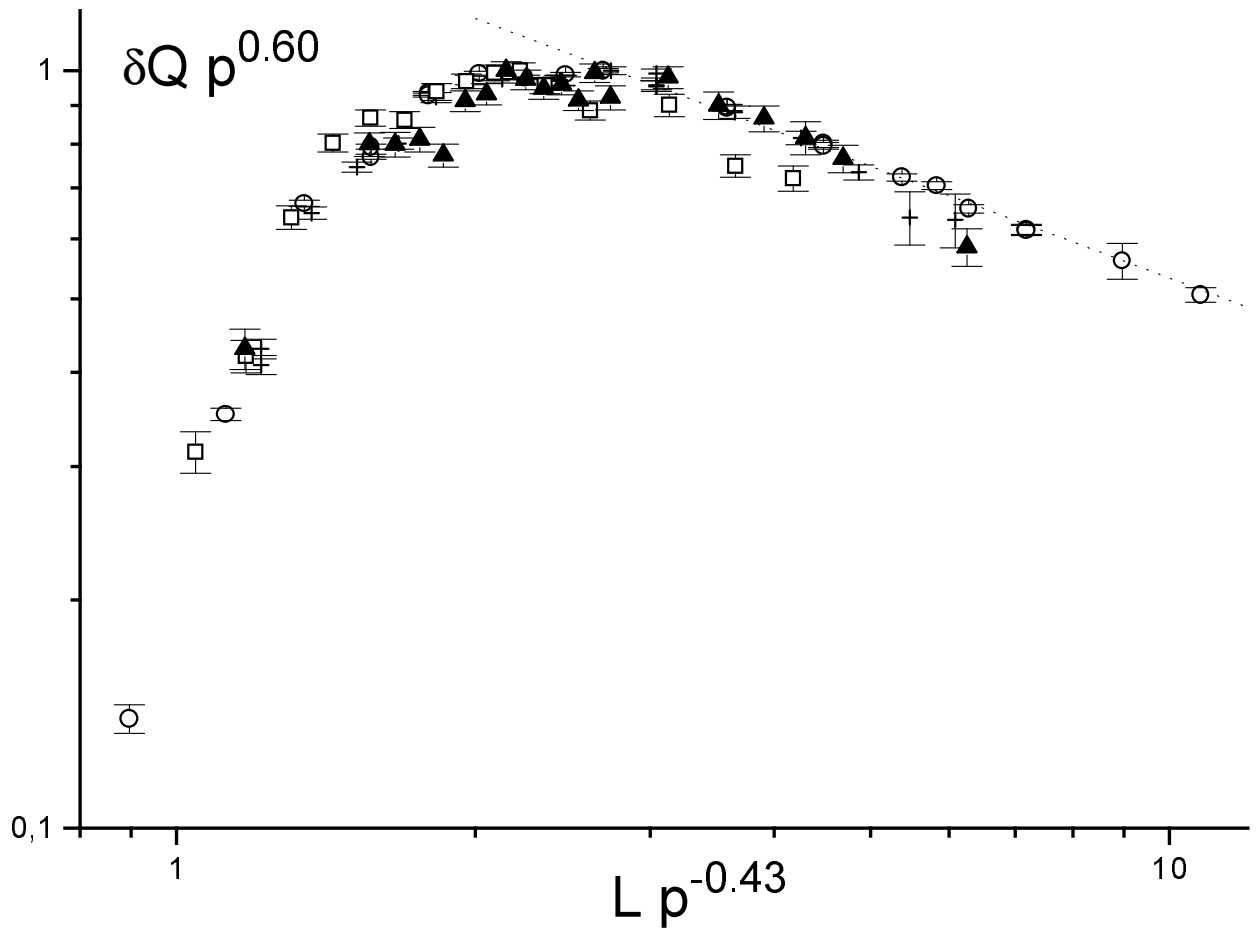


FIG. 4. Scaled deviation of dimensionless ratio δQ versus the scaled system size, for several SR. The symbols are defined in the caption to Fig. 1.